Article

Electrochemiluminescence Detection of Escherichia coli O157:H7 Based on a Novel Polydopamine Surface Imprinted Polymer Biosensor

Shufan Chen, Xueqian Chen, Lijuan Zhang, Juanjuan Gao, and Qiang Ma

ACS Appl. Mater. Interfaces, **Just Accepted Manuscript** • DOI: 10.1021/acsami.6b12455 • Publication Date (Web): 18 Jan 2017

Electrochemiluminescence Detection of *Escherichia coli* O157:H7 Based on a Novel Polydopamine Surface Imprinted Polymer Biosensor

Shufan Chen[a], Xueqian Chen[a], Lijuan Zhang[b], Juanjuan Gao[c], Qiang Ma[a*]

[a] *Department of Analytical Chemistry, College of Chemistry, Jilin University, Changchun, 130012, China*

[b] *State Key Laboratory for Supramolecular Structure and Materials, College of Chemistry, Jilin University, Changchun, 130012, China*

[c] *State Key laboratory of Inorganic Synthesis and Preparative Chemistry, College of Chemistry, Jilin University, Changchun 130012, China.*

*Corresponding author

Tel.: +86-431-85168352

E-mail address: *Qma@jlu.edu.cn*

Abstract

In this paper, a facilely prepared electrochemiluminescence (ECL) biosensor was developed for Escherichia coli (*E. coli)* O157:H7 quantitative detection based on polydopamine (PDA) surface imprinted polymer (SIP) and nitrogen-doped graphene quantum dots (N-GQDs). N-GQDs with a high quantum yield of 43.2% were synthesized. The uniform PDA SIP film for *E. coli* O157:H7 was established successfully with a facile route. The dopamine and the target bacteria were electropolymerized directly on the electrode. After removed *E. coli* O157:H7 template, the established PDA SIP can selectively recognize *E. coli* O157:H7. Accordingly, *E. coli* O157:H7 polyclonal antibody (pAb) was labeled with N-GQDs. The bioconjugation of SIP-*E. coli* O157:H7/pAb-N-GQDs can generate intensive ECL irradiation with $K_2S_2O_8$. As a result, *E. coli* O157:H7 was detected with the ECL sensing system. Under optimal conditions, the linear relationships between the ECL intensity and *E. coli* O157:H7 concentration was obtained from 10^1 colony-forming unit (CFU) mL^{-1} to 10^7 CFU mL^{-1} with a limit of detection (LOD) of 8 CFU mL^{-1}. And the biosensor based on this SIP film has been applied in the water samples detection successfully. The N-GQDs based ECL analytical method for *E. coli* O157:H7 was reported for the first time. The sensing system had high selectivity to the target analyte and provided new opportunities, and speed up disease diagnosis, treatment and prevention with pathogen.

Keywords: Surface imprinted polymer, electrochemiluminescence, *E. coli* O157:H7, nitrogen-doped graphene quantum dot, dopamine, electropolymerization.

Introduction

Bacteria exist in nature environment widely, such as water and food. Among the various bacteria, the pathogenic bacteria at infinitesimal amounts can seriously affect public health. For example, *E. coli* O157:H7 can cause serious illnesses, e.g. hemorrhagic colitis (HC) and hemolytic uremic syndrome (HUS). *E. coli* O157:H7 is one of the most dangerous types pathogenic bacteria especially in young and immunocompromised individuals.[1] Conventional detection methods for pathogenic bacteria include culture techniques and polymerase chain reaction (PCR). However, these methods require substantially time-consuming, skilled technical staff and expensive equipment.[2] Therefore, it is important to develop new methods that can detect *E. coli* O157:H7 more accurately and sensitively.[3-11]

Electrochemiluminescence (ECL) have become a hot topic in analytical technique research with both the simplicity of electrochemistry and high sensitivity of the chemiluminescence method.[12] Therefore, ECL is receiving more and more attention, and becoming a powerful sensing technique owing to the low background interference, rapid response, and excellent sensitivity.[13] Various chemical and biological sensing systems were fabricated based on ECL and nanoparticles.[14-16] But there existed no ECL biosensor for *E. coli* O157:H7 until now. Graphene quantum dots (GQDs) are ideal carbon nanomaterial due to its unique properties.[17] Because of quantum confinement and edge effects, GQDs have fascinating characteristics, including photo induced electron transfer, photoluminescence, and especially the ECL performance.[18,19] Furthermore, doping GQDs with substituent N heteroatoms drastically alter electro-optical properties of GQDs and could produce unexpected properties. For example, the synthetic N-GQDs have abundant carboxy groups and exhibit strong ECL activity with $K_2S_2O_8$ as coreactant on the GCE.[18] Molecularly imprinted polymers (MIPs) can recognize target molecules with highly specific ability.[20] The tailor-made binding sites in the MIPs are complementary in shape, size to the template analyte.[21] MIPs have been widely used in the detection of simple organic molecule,[22, 23] protein[24,25], and antibody-free biomarker[26]. Now, the concept

of molecular imprinting has been extended toward surface imprinting polymers (SIPs) [10]. The template analytes in SIPs research have covered macromolecular, cell and bacteria.[10,27-31] However, we found that there existed few SIPs-based analytical methods for *E. coli* O157:H7 among the abundant reported SIPs sensors. So, it is necessary to fabricate high sensitive SIPs biosensors for sensing *E. coli* O157:H7.

Dopamine (DA) is a functional biomolecule in mussel adhesive proteins. DA can polymerize and form adherent polydopamine (PDA) at alkaline pH. PDA have been used and in various surfaces of nanoparticles, films, microspheres and so on .[32] PDA film formed by electrochemical oxidation is a biocompatible matrix for the biomolecules immobilization.[33] And PDA-modified surfaces can resist nonspecific absorption.[34] On the basis of the ECL characteristics of N-GQDs and high selectivity of SIPs, a novel bisensor for *E. coli* O157:H7 was presented in this work. Scheme 1 described the *E. coli* O157:H7 sensing process of PDA SIP-based ECL platform. In the co-polymerization of DA, the target bacteria worked as template in the formed PDA film on the electrode surface. After the template was removed, a PDA SIP can be obtained. The PDA SIP can recognize and combine the target bacteria. On the other side, polyclonal antibody (pAb) to *E. coli* O157:H7 can be labeled with N-GQDs activated by EDC. Subsequently, the specific binding between the pathogenic bacteria and pAb on the modified GCE can generate ECL signal with $K_2S_2O_8$ electrolyte. The proposed sensor possessed three main features: (i) a rigid, uniform PDA imprinted film was prepared via facile electropolymerization method; (ii) the obtained PDA SIP had high selectivity to the target analyte; and (iii) the ECL method with N-GQDs was employed for *E. coli* O157:H7 detection, and the proposed method have the potential application on the determination of other bacteria.

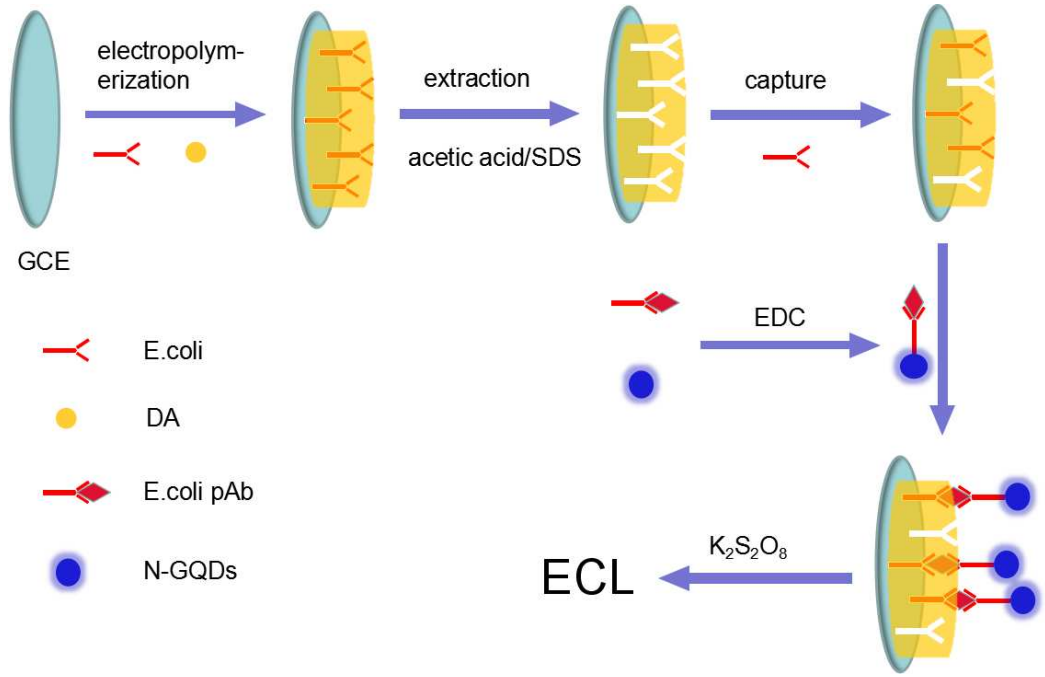

Scheme 1. Schematic presentation of fabrication procedure of biosensor and detection process.

Experiment section

Materials. 1-ethyl-3-(3-dimethylamino-propyl) carbodiimide (EDC, analytical grade), threonine (analytical grade), glycine, arginine (analytical grade), histidine (analytical grade), dopamine (DA, analytical grade), NaOH, Na_3PO_4, Na_2HPO_4, NaH_2PO_4, acetic acid, Critic acid, ammonia (30% wt), and sodium dodecyl sulfate (SDS) were purchased from Sigma-Aldrich and Dingguo Co. *E. coli* O157:H7 and the polyclonal antibody (pAb) were purchased from Shanghai Linc-Bio Science Company, Ltd. We collected the water samples form Jilin University water tap. Transmission electron microscopy (TEM) images of N-GQDs were obtained with a Philips Tecnai F20 TEM. The electrochemical data were recorded with a CHI 660B electrochemical workstation with a three-electrode system. Optical and ECL signals were recorded by UV-vis spectrophotometer, spectrofluorophotometer and ultraweak luminescence instrument, respectively.

Preparation of N-GQDs and quantum yield (QY) measurement. N-GQDs were synthesized through hydrothermal treatment of critic acid and ammonia

according to the previous report.[35,36] The mixture of 2g critic acid and 0.3 mL ammonia were heated at 210 ^{o}C for 1 h. After cooling to the room temperature, the obtained mixture was ultrasounded and dissolved in water. The acidity of the N-GQDs dispersion was regulated to pH 7.0 by using NaOH solution. In the purification step, the N-GQDs were washed via centrifugation at 12,000 rpm. Finally, N-GQDs was diluted to 20 mL water with a precise concentration at 5 mg/mL.

The QY of the resultant N-GQDs was calculated according to the follow equation:[37]

$$Y_u = Y_s \frac{I_u}{I_s} \frac{A_s}{A_u} \frac{{n_u}^2}{{n_s}^2} \qquad (1)$$

where *Y* represents the quantum yield. *I* represents the measured integrated emission intensity. .*A* is the absorbance intensity. *n* is the refractive index of the solvent. "u" represent the N-GQDs. And "s" represent quinine sulfate (QY 0.54) standard sample.

Fabrication of PDA SIP. Prior to modification, 5 mmol/L DA and 10^8 CFU/mL *E. coli* O157:H7 in the pH 7.4 phosphate buffer were bubbled with high purified nitrogen for 15 min to remove oxygen. Then the clean electrode was immersed in the solution. 30 cycles cyclic voltammetry (-0.5~0.5 V) were performed to form the PDA SIP. The scan rate was 0.02V/s. The modified PDA SIP was washed with ultrapure water and immersed in 5% wt acetic acid/SDS solution for 18 h to remove bacteria template.

ECL Detection. The mixture of 1.5 mg N-GQDs and 300 μL of 100 mmol L^{-1} EDC were incubated at 25^{o}C for 20 min. Then 20 μL of 50 μg mL^{-1} pAb was added into the mixture solution and incubated for 2 h. Then, the N-GQDs labeled pAb were obtained. After centrifuged and washed, the resultant N-GQDs-pAb was dispersed with PBS to a final volume of 1.0 mL for further use. PDA SIP modified electrode was immersed into the *E. coli* O157:H7 standard solution for 20 min. The electrode was washed with water to remove the unbound *E. coli* O157:H7. The modified electrode then was immersed into N-GQDs-pAb solution and incubated for 2 h at 37 ^{o}C. Subsequently, excess N-GQDs-pAb was washed off with water. The ECL signal

was collected in 10 mmol L^{-1} PBS containing 0.1 mol L^{-1} $K_2S_2O_8$ under the cyclic voltammetry from 0 to -2.0 V.

Results and discussion

Characterization of N-GQDs. Transmission electron microscopy (TEM) image in Fig. 1 showed the N-GQDs were well monodispersed and uniform. In this work, N-GQDs had ca. 4nm size and a high quantum yield of 43.2%. FT-IR spectra (Fig. S1A) were used to demonstrate the N-GQDs surface state. The stretching vibrations of O-H and N-H at 3425 and 3201 cm^{-1} absorption bands, the bending vibration of C-NH at 1377 cm^{-1} peak, the C=O vibration at 1700 cm^{-1} absorption band, and the C-OH stretching vibrations at 1177 and 1225 cm^{-1} peaks implied that the N-GQDs have nitrogen containing structure and oxygen-enriching property. [38] Under maximum excitation wavelength (ca. 353 nm), the N-GQDs had an emission peak at 440 nm (shown in Fig. S1B). The UV-vis absorption and fluorescence emission spectra at different excitation wavelengths were recorded in Fig. S1C. There was an obvious UV-vis absorbance band at 334 nm due to n-π^* transition of C=O bone of N-GQDs.[39] The fluorescence emission spectra depicted in Fig. S1C processed a typical excitation-dependent feature.[37] The emission peak gradually red-shift (440-540 nm) with varying excitation wavelengths (330-480 nm). The elemental composition of N-GQDs were further discussed in Fig. S2. The full range of XPS analysis showed three peaks at 284.6, 400.8, and 531.3 eV. The peaks were attributed to C 1s, N 1s, and O 1s, respectively.[30] And Fig. S2 C showed there were two deconvoluted peaks (assigned to C-N-C and N-$(C)_3$) groups in the high-resolution N 1s spectrum. Fig. S2 D indicated the fitted peaks (assigned to C=O, C-OH, and 1C-O-C groups) in the O 1s spectrum. The above XPS indicated that the N-GQDs have multiple oxygenated and nitrous groups.[40]

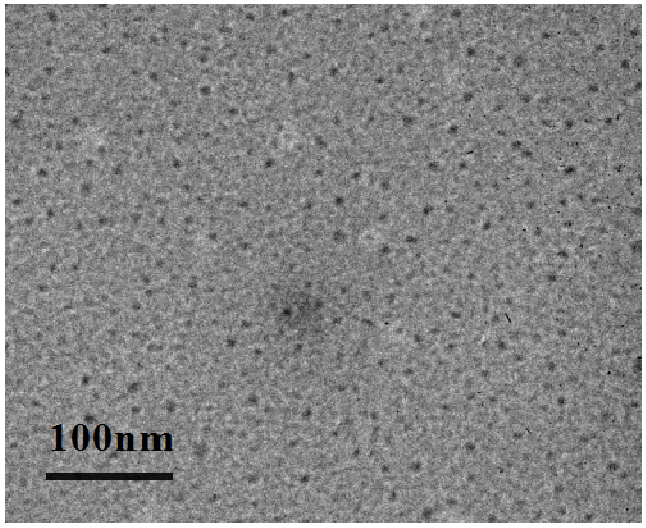

Fig. 1. TEM photograph of the nitrogen-doped GQDs.

Preparation of PDA SIP. PDA imprinted film was prepared through the electropolymerization method. In general, the electropolymerization method was employed to form homogeneous polymer film on the electrode surface.[41] The shape, size and thickness of the imprinted polymer film can be easily controlled via the deposition conditions.[22,42] Fig. 2 showed CV curves recorded during the co-polymerization process of DA and *E. coli* O157:H7 pathogenic bacteria. In the first CV scan, an oxidation peak at +0.27 V demonstrated the oxidation of DA to dopaminequinone. And two cathodic peaks appeared at +0.13 V and -0.25 V in the first negative scan were associated to the reduction of dopaminequinone and dopaminechrome, respectively. A oxidation peak at -0.20 V in the second positive scan was associated to the oxidation of leucodopaminechrome.[43,44] The peak currents decreased indicated that the formation of a compact film progressively covered the electrode surface.[22,45] Moreover, the CV curves had no significant difference when the electropolymerization carried out without *E. coli* O157:H7. These results suggest that the target bacteria did not have electroactivity on the GCE. In the process of co-polymerization, *E. coli* O157:H7 can be bound via hydrogen bond in the PDA chain which had much amino-group. So there was a three dimensional matrix for binding *E. coli* O157:H7 based on the cross-linking of PDA. After bacteria template were removed, the imprinted cavities were created in PDA, which can recognize *E.*

coli O157:H7 via the shape and size selection.[24] As a result, PDA SIP was prepared successfully.

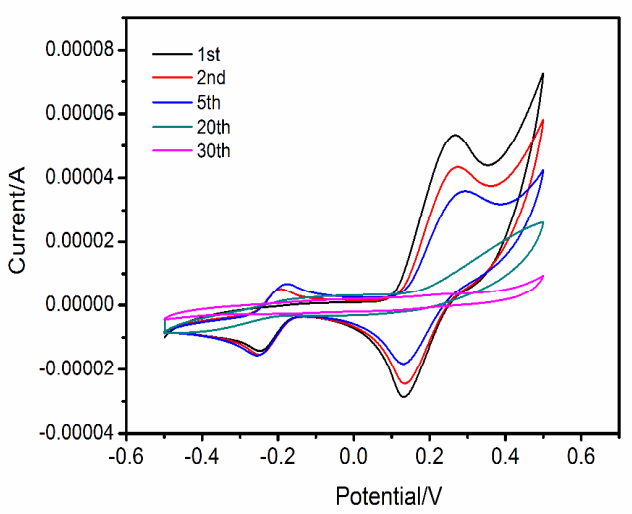

Fig. 2. Cyclic voltammetry for the dopamine electropolymerization with *E. coli* O157:H7 on GCE. Scan rate: 0.02V/s

Electrochemical properties of the modified electrode and characterization of N-GQDs labeled pAb. To investigate the changes of electrode behavior after each assembly step, CV was performed with a supporting electrolyte of 0.1 mol L^{-1} KCl and 1.0 mmol L^{-1} $K_3[Fe(CN)_6/K_4[Fe(CN)_6]$. As shown in Fig. 3A, obvious redox peaks can be found in the CV of bare GCE (curve a). After the electropolymerization of DA and *E. coli* O157:H7, redox peaks (curve b) disappeared indicating the successful coating on the GCE of the PDA SIP. From curve c, the PDA SIP modified electrode showed an increase of current response after the removal of *E. coli* O157:H7. It was because more imprinted cavities in the SIP film, more $Fe(CN)^{3-/4-}$ penetration channels for electrochemical redox. After the pathogenic bacteria were captured by the SIP film, there was an obvious decrease in current peak in curve d due to the rebinding of bacteria in cavities.

EIS provided the impedance changes on the electrode in the modification process.[41] As shown in Fig. 3B, the cleaned electrode (curve a) showed a mass diffusion limiting process. And the impedance of PDA film and PDA SIP modified electrode were found. There were obvious increase at 1862 Ω (curve b) and 3969 Ω

(curve c) when PDA film was formed on the GCE without and with the presence of bacteria, respectively. It indicated that *E. coli* O157:H7 has been embedded into the PDA matrix and SIP was prepared successfully. This phenomenon indicated that the PDA can decrease the electron transfer rate, which had large obstruction effect. Without *E. coli* O157:H7, the generation of imprinted cavities increased the electron transfer and decreased the diameter of the semicircle of EIS to about 1465 Ω (curve d). Subsequently, when *E. coli* O157:H7 was captured, the impedance of SIP-based electrode had an apparent enhancement (curve e). Finally, when the N-GQDs labeled pAb (pAb-N-GQDs) was modified on the SIP via the specific binding with *E. coli* O157:H7 (labeled as SIP-*E. coli* O157:H7/pAb-N-GQDs), the impedance increased (curve f) to 2219 Ω. The increase showed the hindrance effect of N-GQDs and pAb to the electrical conductivity. The EIS characterized the stepwise modification of the electrode. To further demonstrated the fabrication of the PDA SIP, photomicrographs of the bare GCE and PDA SIP modified GCE were taken in the study. The result showed in the inset of Fig. S3B. It can be seen that after the electropolymerization, uniform PDA SIP was formed on the surface of GCE. In order to certify bacteria template has been removed completely from the PDA SIP, we measured the UV-vis absorption curves (showed in Fig. S3) in the extraction process. Solution a (curve a) was the acetic acid/SDS solution with the removed the target bacteria from PDA SIP after the extraction time of 18 h. Solution b (curve b) was acetic acid/SDS solution with the outer addition of standard solution *E. coli* O157:H7 (10^8 CFU mL^{-1}). The small difference in the absorbance intensity of acetic acid/SDS solution can certify that the most *E. coli* O157:H7 in PDA SIP has been extracted.

UV-vis absorption and fluorescence spectra were collected to characterize the N-GQDs labeled pAb (pAb-N-GQDs). As shown in Fig. S4A, it can be observed that there existed two obvious absorption bands in the pAb-N-GQDs. And the absorance band at 275 nm can be ascribed to the absorption of pAb which has combined to the surface of N-GQDs. Fig. S4B showed the photoluminescence spectra of N-GQD and pAb-N-GQDs. And we can found that the fluorescence intensity of N-GQDs had a decline after binding with pAb.

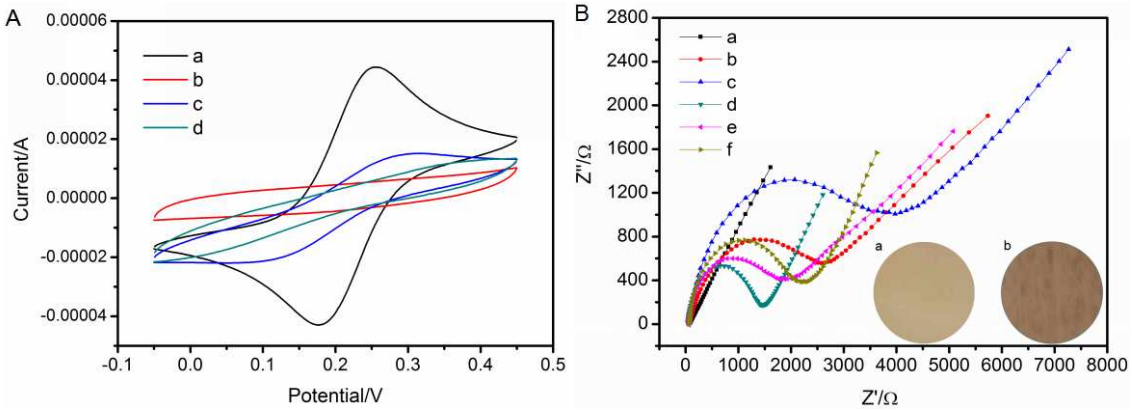

Fig. 3. (A) CV curves of different modified electrode: (a) bare GCE; (b) PDA SIP coated electrode; (c) PDA SIP modified electrode after the removal of pAb and (d) SIP-*E. coli* O157:H7 modified electrode. (B) EIS of (a) cleaned GCE; (b) PDA modified electrode without the presence *E. coli* O157:H7; (c) PDA SIP coated electrode; (d) PDA SIP coated electrode after the removal of *E. coli* O157:H7; (e) SIP-*E. coli* O157:H7; (f) SIP-*E. coli* O157:H7/pAb-N-GQDs. The concentration of *E. coli* O157:H7: 10^4 CFU mL^{-1}. Inset: Photomicrographs of cleaned GCE (a), and PDA SIP modified GCE (b).

ECL behavior and condition optimization. To generate ECL signal, pAb-N-GQDs was bound to the SIP-*E. coli* O157:H7 modified electrode based on the antigen-antibody reaction. The mechanism for ECL generation was according to the equations below:

$$N-GQDs+e^- \rightarrow N-GQDs^{\bullet-} (2)$$

$$S_2O_8^{2-}+e^- \rightarrow SO_4^{2-}+SO_4^{\bullet-} (3)$$

$$N-GQDs^{\bullet-}+SO_4^{\bullet-} \rightarrow N-GQDs^{*}+SO_4^{2-} (4)$$

$$N-GQDs^{*} \rightarrow N-GQDs+h\nu (5)$$

Furthermore, the optimal pH value and incubation time for the immunoreaction of the target bacteria and antibody was investigated. The SIP-bacteria modified electrode was then immersed with pAb-N-GQDs in different pH value PBS. As shown in Fig. S5A, the ECL intensity of the SIP based sensing system increased when the pH value up to 8.0. The results showed that *E. coli* O157:H7 can connect more pAb at pH 8.0 and then produced higher ECL signal due to the introduction of more N-GQDs.

Therefore, pH 8.0 was selected as the optimal pH. As displayed in Fig. S5B, followed the increasing incubation time, the ECL intensity increased rapidly within 2 h. Therefore, 2 h incubation time were employed in the following detection process.

The determination of *E. coli* O157:H7. The quantitative measurements of the target bacteria were carried out with the prepared SIP based biosensor. With the increasing concentration of target bacteria bound into the imprinted cavities, more pAb-N-GQDs can be introduced to the electrode and further promoted the occurrence of more N-GQD*. As shown in Fig. 4A, the ECL intensity increased gradually with the increasing bacteria concentration from 10^1 CFU mL^{-1} to 10^7 CFU mL^{-1} under the optimal experimental conditions (Fig. 4B). The regression equation was $I=1128.5+891.6 \lg c_{E.coli}$ with a correlation coefficient (R) of 0.998. The detection limit (LOD) was 8 CFU mL^{-1}. Then continuous increase of ECL signal was observed.

To investigate the recognition specificity of the SIP toward *E. coli* O157:H7, we recorded the ECL signal with the addition of *Salmonella* as a comparison. As shown in Fig. S6, it can be seen that there was no obvious ECL signal enhancement. It indicated that the prepared SIP has good selectivity for *E. coli* O157:H7. In the sensing system, even though few other bacteria could be captured by the SIP, the specific immunoreaction between *E. coli* O157:H7 and pAb-N-GQDs ensure the proposed biosensor high selectivity. So there was no ECL signal in control-experiment. Subsequently, in order to illustrate the validity of the ECL biosensor for *E. coli* O157:H7, interference experiments were carried out. Table S1 showed the results of interference effect with a relative error of ± 5.0%. 500 μmol L^{-1} for Na^+, K^+, Ca^{2+}, Mg^{2+}, 100 μmol L^{-1} for threonine, glycine, arginine, and histidine, and 10^4 CFU mL^{-1} of Salmonella have almost no interference on the *E. coli* O157:H7 detection. With these commonly existing ions, amion acid and other bactria, there was little interference on the detection of the target bacteria. In addition, in order to evaluate the feasibility of the proposed SIP biosensor, water samples with spiking *E. coli* O157:H7 were detected. Table 1 showed the quantitative recoveries of the spiked *E. coli* O157:H7 were in the range of 0.994-1.02. The comparison of other detection methods was summed up in Table S2. It showed that the proposed ECL biosensor for

E. coli O157:H7 detection had a much wider linearity range and a lower LOD comparing with other sensing systems.

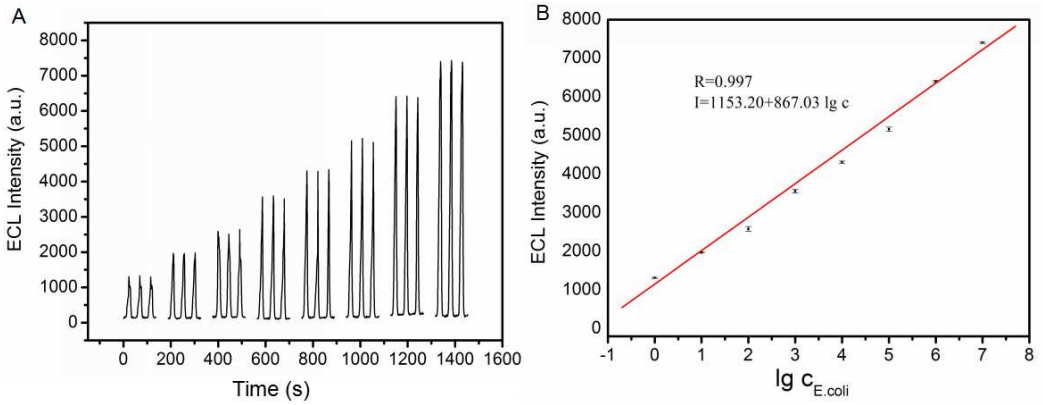

Fig. 4. (A) ECL time trace to different concentration of the target bacteria (from left to right: 10^1, 10^2, 10^3, 10^4, 10^5, 10^6, 10^7 CFU mL^{-1}). (B) Calibration curve for quantification of *E. coli* O157:H7.

Table 1 The determination of *E. coli* O157:H7 in water samples

Samples	Added (CFU/mL)	Found (CFU/mL)	Recovery	RSD (%)
1	5.00×10^1	5.09×10^1	1.02	2.31
2	5.00×10^2	4.97×10^2	0.994	1.78
3	5.00×10^4	4.99×10^4	0.998	1.39

Conclusion

A novel SIP biosensor has been developed through the facile electropolymerization method and detected *E. coli* O157:H7 via the ECL signal of N-GQDs with $K_2S_2O_8$ as the coreactant. The established SIP can specifically capture and selectively recognize the target pathogenic bacteria. The electrochemical properties of the modified electrode were studied by collecting the EIS and CV stepwise. 10^1-10^7 CFU mL^{-1} *E. coli* O157:H7 can be detected. This was the first time that *E. coli* O157:H7/SIP based ECL method was reported. Most importantly, not only this work determined the *E. coli* O157:H7 in water samples successfully, but also have the potential application for analysis of other bacteria.

Associated content

Supporting information

FT-IR spectrum, fluorescence spectra, UV-vis absorption spectra, and XPS spectrum of N-GQDs. UV-vis absorption of PDA SIP and the target bacteria. UV-vis spectra and fluorescence spectra of *E. coli* O157:H7-N-GQDs. Effect of incubation pH and incubation time. Selectivity of the ECL biosensor. The interference of the coexisting substances on the determination of *E. coli* O157:H7. Comparison of different methods for the detection of *E. coli* O157:H7. This material is available free of charge via the internet at http://pubs.acs.org.

Acknowledgments

This work was financially supported by the National Nature Science Foundation of China (No. 21075050 and 21005029) and Youth Science Fund of Jilin Province (20140520081JH).

References

(1) Hu, R.; Yin, Z.; Zeng, Y.; Zhang, J.; Liu, H.; Shao, Y.; Ren, S.; Li, L. A Novel Biosensor for Escherichia coli O157:H7 Based on Fluorescein-Releasable Biolabels. *Biosens. Bioelectron.* 2016, 78, 31-36.

(2) Zhang, Y.; Tan, C.; Fei, R.; Liu, X.; Zhou, Y.; Chen, J.; Chen, H.; Zhou, R.; Hu, Y. Sensitive Chemiluminescence Immunoassay for E. coli O157:H7 Detection with Signal Dual-Amplification Using Glucose Oxidase and Laccase. *Anal. Chem.* 2014, 86, 1115-1122.

(3) Magliulo, M.; Simon, P.; Guardigli, M.; Michelini, E.; Luclani, M.; Lelli, R.; Roda, A. A. A Rapid Multiplexed Chemiluminescent Immunoassay for the Detection of Escherichia coli O157:H7, Yersinia Enterocolitica, Salmonella Typhimurium, and Listeria Monocytogenes Pathogen Bacteria. *J. Agric. Food Chem.* 2007, 55, 4933-4939.

(4) Li, F.; Zhao, Q.; Wang, C.; Lu, X.; Li, X.; Le, C. X. Detection of Escherichia coli O157:H7 Using Gold Nanoparticles Labeling and Inductively Coupled Plasma Mass Spectrometry. *Anal. Chem.* 2010, 82, 3399-3403.

(5) Liao, W.; Ho, A. J. Attomole DNA electrochemical Sensor for the Detection of Excherichia coli O157. *Anal. Chem.* 2009, 81, 2470-2476.

(6) Li, Y.; Fang, L.; Cheng, P.; Deng, J.; Jiang, L.; Huang, H.; Zheng, J. An Electrochemical Immunosensor for Sensitive Detection of Escherichia coli O157:H7 Using C_{60} Based Biocompatible Paltform and Enzyme Functionalized Pt Nanochains Tracing Tag. *Biosens. Bioelectron.* 2013, 49, 485-491.

(7) Song, C.; Liu, J.; Li, J.; Liu, Q. Dual FITC Lateral Flow Immunoassay for Sensitive Detection of Escherichia coli O157:H7 in Food Samples. *Biosens. Bioelectron.* 2016, 85, 734-739.

(8) Hussein, A.; Hassan, A.; Escosura-Muñiz, A.; Merkoçi, A. Highly Sensitive and Rapid Determination of Escherichia coli O157:H7 in Minced Beef and Water Using Electrocatalytic Gold Nanoparticle Tags. *Biosens. Bioelectron.* 2015, 67, 511-515.

(9) Zhang, L.; Huang, Y.; Wang, J.; Rong, Y.; Lai, W.; Zhang, J.; Chen, T. Hierarchical Flowerlike Gold Nanoparticles Labeled Immunochromatography Test Strip for Highly Sensitive Detection of Escherichia coli O157:H7. *Langmuir* 2015, 31, 5537-5544.

(10) Grinsven, V. B.; Eersels, K.; Akkermans, O.; Ellermann, S.; Kordek, A.; Peeters, M.; Deschaume, O.; Bartic, C.; Diliën, H.; Redeker, S. E.; Wagner, P.; Cleij, J. T. Label-Free Detection of Escherichia coli Based on Thermal Transport through Surface Imprinted Polymers. *ACS Sens.* 2016, 1, 1140-1147.

(11) Abdalhai, H. M.; Fernandes, A.; Xia, X.; Musa, A.; Ji, J.; Sun, X. Electrochemical Genosensor to Detect Pathogenic Bacteria (E. coli O157:H7) as Applied in Real Food Samples (Fresh Beef) to Improve Food Safety and Quality Control. *J. Agric. Food. Chem.* 2015, 63, 5017-5025.

(12) Liu, L.; Ma, Q.; Li, Y.; Liu, Z.; Su, X. A Novel Signal-Off Electrochemiluminescence Biosensor for the Determination of Glucose Based on Double Nanoparticles. *Biosens. Bioelectron.* 2015, 63, 519-524.

(13) Chen, S.; Chen, X.; Xia, T.; Ma, Q. A Novel Electrochemiluminescence Sensor

for the Detection of Nitroaniline Based on the Nitrogen-Doped Graphene Quantum Dots. *Biosens. Bioelectron.* 2016, 85, 903-908.

(14) Zhao, L.; Li, J.; Liu, Y.; Zhang, W.; Zhang, J.; Xia, Q.; Zhang, Q.; Zhao, W.; Chen, X. A Novel ECL Sensor for Determination of Carcinoembryonic Antigen Using Reduced Graphene Oxide-$BaYF_5$:Yb, Er Upconversion Nanocomposites and Gold Nanoparticles. *Sens. Actuators, B* 2016, 232, 484-491.

(15) Stewart, J.A.; OReilly, E.; Moriarty, D.R.; Bertoncello, P.; Keyes, E.T.; Forster, J.R.; Dennany, L. A Cholesterol Biosensor Based on the NIR Electrogenerated-Chemiluminescence (ECL) of Water-Soluble CdSeTe/ZnS Quantum Dots. *Electrochim. Acta* 2015, 157, 8-14.

(16) Huang, T.; Meng, Q.; Jie, G. Silver Nanowires-Based Signal Amplification for CdSe Quantum Dots Electrochemiluminescence Immunoassay. *Biosens. Bioelectron.* 2015, 66, 84-88.

(17) Li, N.; Jia, L.; Ma, R.; Jia, W.; Lu, Y.; Shi, S.; Wang, H. A Novel Sandwiched Electrochemiluminescence Immunosensor for the Detection of Carcinoembryonic Antigen Based on Carbon Quantum Dots and Signal Amplification. *Biosens. Bioelectron.* 2016, 89, 453-460.

(18) Han, T.; Yan, T.; Li, Y.; Cao, W.; Pang, X.; Huang, Q.; Wei, Q. Eco-Friendly Synthesis of Electrochemiluminescent Nitrogen-Doped Carbon Quantum Dots From Diethylene Triamine Pentacetate and Their Application for Protein Detection. *Carbon* 2015, 91, 144-152.

(19) Zhang, L.; Li, L.; Ma, C.; Ge, S.; Yan, M.; Bian, C. Detection of α-Fetoprotein with an Ultrasensitive Electrochemiluminescence Paper Device Based on Green-Luminescent Nitrogen-Doped Graphene Quantum Dots. *Sens. Actuators, B* 2015, 221, 799-806.

(20) Kuwata, T.; Uchida, A.; Takano, E.; Kitayama, Y.; Takeuchi, T. Molecularly Imprinted Polymer Arrays as Synthetic Protein Chips Prepared by Transcription-Type Molecular Imprinting by Use of Protein-Immobilized Dots as Stamps. *Anal. Chem.* 2015, 87, 11784-11791.

(21) Chen, L.; Wang, X.; Lu, W.; Wu, X.; Li, J. Molecular Imprinting: Perspectives

and Applications. *Chem. Soc. Rev.* 2016, 45, 2137-2211.

(22) Liu, K.; Wei, W.; Zeng, J.; Liu, X.; Gao, Y. Application of a Novel Electrosynthesized Polydopamine-Imprinted Film to the Capacitive Sensing of Nicotine. *Anal. Bioanal. Chem.* 2006, 385, 724-729.

(23) Hu X.; Xie L.; Guo J.; Li H.; Jiang X.; Zhang Y.; Shi S. Hydrophilic Gallic Acid-Imprinted Polymers over Magnetic Mesoporous Silica Microspheres with Excellent Molecular Recognition Ability in Aqueous Fruit Juices. *Food Chem.* 2015, 179, 206–212.

(24) Li, L.; Fan, L.; Dai, Y.; Kan, X. Recognition and Determination of Bovine Hemoglobin Using a Gold Electrode Modified with Gold Nanoparticles and Molecularly Imprinted Self-Polymerized Dopamine. *Microchim. Acta* 2015, 182, 2477-2483.

(25) Whitcombe, J. M.; Chianella, I.; Larcombe, L.; Piletsky, A. S.; Noble, J.; Poter, R.; Horgan, A. The Rational Development of Molecularly Imprinted Polymer-Based Sensors for Protein Detection. *Chem. Soc. Rev.* 2011, 40, 1547-1571.

(26) Rossetti, C.; Qader, A. A.; Halvorsen, G. T.; Sellergren, B.; Reubsaet, L. Antibody-Free Biomarker Determination: Exploring Molecularly Imprinted Polymers for Pro-Gastrin Releasing Peptide. *Anal. Chem.* 2016, 84, 12291-12298.

(27) Aherne, A.; Alexander C.; Payne, J. M.; Perez, N.; Vulfson, N. E. Bacteria-Mediated Lithography of Polymer Surfaces. *J. Am. Chem. Soc.* 1966, 118, 8771-8772.

(28) Schirhagl, R.; Hall, W. E.; Fuereder, I.; Zare, N. R. Seperation of Bacteria with Imprinted Polymeric Films. *Analyst* 2012, 137, 1495-1499.

(29) Ren, K,; Zare, N. Chemical Rocogintion in Cell-Imprinted Polymers. *ACS Nano* 2012, 6, 4314-4318.

(30) Eersels, K.; Grinsven, V. B.; Khorshid, M.; Somers, V.; Püttmann, G.; Stein, C.; Barth, S.; Diliën, H.; Bos, M. G.; Germeraad, T. W.; Cleij, J. T.; Thoelen, R.; Ceuninck, D. W.; Wagner, P. Heat-Transfer-Method-Based Cell Culture Quality Assay through Cell Detection by Surface Imprinted Polymers. *Langmuir* 2015, 31, 2043-2050.

(31) Dickert, F. L.; Hayden, O. Bioimprinting of Polymers and Sol-Gel Phases. Selective Detection of Yeasts with Imprinted Polymers. *Anal. Chem.* 2002, 74, 1302-1306.

(32) Yari, A.; Derki, S. New MWCNT-Fe_3O_4@PDA-Ag Nanocomposite as a Novel Sensing Element of an Electrochemical Sensor for Determination of Guanine and Adenine Contents of DNA. *Sens. Actuators, B* 2016, 227, 456-466.

(33) Ruan, C.; Shi, W.; Jiang, H.; Sun, Y.; Liu, X.; Zhang, X.; Sun, Z.; Dai, L.; Ge, D. One-Pot Preparation of Glucose Biosnsor Based on Polydopamine-Graphene Composite Film Modified Enzyme Electrode. *Sens. Actuators, B* 2013, 177, 826-832.

(34) Zhang, Y.; Geng, X.; Ai, J.; Gao, Q.; Qi, H.; Zhang, C. Signal Amplification Detection of DNA Using a Sensor Fabricated by One-Step Covalent Immobilization of Amino-Terminated Probe DNA onto the Polydopamine-Modified Screen-Printed Carbon Electrode. *Sens. Actuators, B* 2015, 221, 1535-1541.

(35) Tam, V. T.; Trung, B. N.; Kim, R. H.; Chung, S. J.; Choi, M. W. One-Pot Synthesis of N-Doped Graphene Quantum Dots as a Fluorescent Sensing Platform for Fe^{3+} Ions Detection. *Sens. Actuators, B* 2014, 202, 568-573.

(36) Dong, Y.; Shao, J.; Chen, C.; Li, H.; Wang, R.; Chi, Y.; Lin, X.; Chen, G. Blue Luminescent Graphene Quantum Dots and Graphene Oxide Prepared by Tuning the Carbonization Degree of Citric Acid. *Carbon* 2012, 50, 4738-4743.

(37) Hu, C.; Liu, Y.; Yang, Y.; Cui, J.; Huang, Z.; Wang, Y,; Yang, L.; Wang, H.; Xiao, Y.; Rong, J. One-Step Preparation of Nitrogen-Doped Graphene Quantum Dots from Oxidized Debris of Graphene Oxide. *J. Mater. Chem. B* 2013, 1, 39-42.

(38) Zhang, H.; Chen, Y.; Liang, M.; Xu, L.; Qi, S.; Chen, H.; Chen, X. Solid-Phase Synthesis of Highly Fluorescent Nitrogen-Doped Carbon Dots for Sensitive and Selective Probing Ferric Ions in Living Cells. *Anal. Chem.* 2014, 86, 9846-9852.

(39) Ju, J.; Zhang, R.; He, S.; Chen, W. Nitrogen-Doped Graphene Quantum Dots-Based Fluorescent Probe for the Sensitive Turn-On Detection of Glutathione and Its Cellular Imaging. *RSC Adv.* 2014, 4,52583-52589.

(40) Zhang, R.; Chen, W. Nitrogen-doped Carbon Quantum Dots: Facile Synthesis and Application as a "Turn-Off" Fluorescent Probe for Detection of Hg^{2+} Ions.

Biosens. Bioelectron. 2014, 55, 83-90.

(41) Amiri, M.; Amali, E.; Nematollahzadeh, A Poly-Dopamine Thin Film for Voltammetric Sensing of Atenolol. *Sens. Actuators, B* 2015, 216, 551-557.

(42) Peng, Y.; Wu, Z.; Liu, Z. An Electrochemical Sensor for Paracetamol Based on an Electropolymerized Molecularly Imprinted *o*-Phenylenediamine Film on a Multi-Walled Carbon Nanotube Modified Glassy Carbon Electrode. *Anal. Methods* 2014, 6, 5673-5681.

(43) Amiri, M.; Amali, E.; Nematollahzadeh, A.; Salehniya, H. Poly-Dopamine Films: Voltammetric Sensor for pH Monitoring. *Sens. Actuators, B* 2016, 228, 53-58.

(44) Li, M.; Deng, C.; Xie, Q.; Yang, Y.; Yao, S. Electrochemical Quartz Crystal Impedance Study on Immobilization of Glucose Oxidase in a Polymer Grown from Dopamine Oxidation at an Au Electrode for Glucose Sensing. *Electrochim. Acta* 2006, 51, 5478-5486.

(45) Wang, J.; Li, B.; Li, Z.; Ren, K.; Jin, L.; Zhang, S.; Chang, H.; Sun, Y.; Ji, J. Electropolymerization of Dopamine for Surface Modification of Complex-Shaped Cardiovascular. *Biomaterials* 2014, 35, 7679-7689.

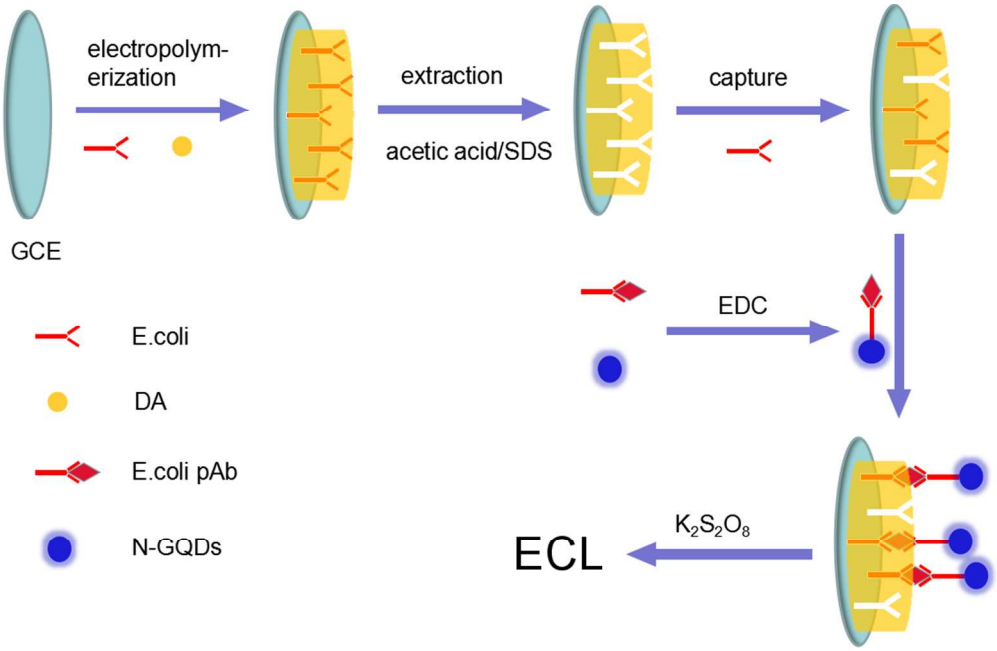

Table of Contents Graphic

299x192mm (96 x 96 DPI)